

Quantum corral wave function engineering

Alfredo A. Correa

Department of Physics, University of California

at Berkeley, Berkeley, California 94720, USA

Lawrence Livermore National Laboratory,

*Livermore, California 94550, USA **

Fernando A. Reboredo

Lawrence Livermore National Laboratory,

Livermore, California 94550, USA †

C. A. Balseiro

Centro Atómico Bariloche Instituto Balseiro,

S.C. de Bariloche, Río Negro 8400, Argentina

(Dated: June 23, 2018)

Abstract

We present a theoretical method for the design and optimization of quantum corrals with specific electronic properties. Taking advantage that spins are subject to a RKKY interaction that is directly controlled by the scattering of the quantum corral, we design corral structures that reproduce spin Hamiltonians with coupling constants determined a priori. We solve exactly the two-dimensional electron gas scattering problem for each corral configuration within the effective mass approximation and s-wave scattering using a Green function method. Subsequently, the geometry of the quantum corral is optimized with an algorithm that combines simulated annealing and genetic approaches. We demonstrate that it is possible to automatically design quantum corrals with complicated target electronic properties, such as multiple mirages with predefined relative intensities at specific locations. In addition we design structures that are particularly sensitive to the phase shift of impurities at certain positions allowing the measurement of the value of this parameter on the copper surface.

PACS numbers:

^{*}Electronic address: correaa@socrates.berkeley.edu

[†]Electronic address: reboredo1@llnl.gov

I. INTRODUCTION

The fabrication of solid state quantum computing devices involves both the ability to manipulate matter at the nanoscale [1] and to design structures that interact according to prescribed quantum computing Hamiltonians[2]. Tuning and controlling quantum interactions are basic problems faced by the quantum computing community. This requires engineering the structure of electronic wave functions in different environments and conditions. The manipulation of individual atoms with STM has made possible the construction of arbitrary quantum structures on top of surfaces. In particular, after the seminal work of Crommie et al.[3], it has been possible to build *quantum corrals* of arbitrary shape, placing atoms one at a time. Quantum corrals are a collection of atoms arranged in a controlled manner on top of a metallic surface. These novel structures generate quantum confinement of the surface conduction electron wave functions leading to striking phenomena such as resonant electronic states and the formation of *quantum mirages* [4]. Generally speaking, quantum mirages are the projection of a perturbation on a point into another distant point of the surface. Manoharan et al.[4] were able to partially project the Kondo [5] electronic structure up to 112Å away from the actual Kondo impurity. In these experiments, the formation of a Kondo mirage relies on the focusing properties of elliptical corrals. These findings triggered a collection of theoretical papers modeling[6, 7, 8] and extending the concept of quantum mirages[9, 10].

This new phenomenon has been proposed as a tool for remote probing [4] and as a way to enhance [8, 9] the interaction between localized magnetic impurities on a surface. Unfortunately, the design of quantum corrals with certain desired properties is still a matter of trial and error[4]. We think that both technological applications and novel physical phenomena could emerge if one could tailor the electronic wave functions that are responsible for the quantum mirage formation. For that purpose we believe that new systematic methods to design quantum corrals are required.

In previous works it was shown that the magnetic interaction between magnetic impurities can be strongly enhanced due to the electronic confinement produced by quantum corrals[8, 9]. Our present objective is to generate the optimal geometrical arrangement of quantum corral atoms that achieves an arbitrary predefined quantum mechanical interaction. This type of problem is usually denoted as *inverse problem*. In contrast to the *direct problem*,

where a physical property is the result of the geometry of the material, in the *inverse problem* the optimized geometry is a result of the physical property targeted. Inverse problems have been addressed in a variety of systems ranging from band gaps of solids [11], design of antennas[12], or intermolecular potential fitting[13]. In order to solve the inverse problem one needs two ingredients: i) a fast method to solve the direct problem (i.e. electron gas response for a given corral configuration) ii) an efficient algorithm to select new configurations and optimize the structure to achieve the target properties.

In this paper we address the ‘inverse quantum corral problem’. We concentrate in the search of structures that could reproduce predefined magnetic Hamiltonians with desired coupling constants by means of an enhanced RKKY interaction. We demonstrate the possibility to physically construct several Hamiltonian examples.

Our theoretical approach consists of i) solving each trial corral configuration with a Green function method[8] and ii) optimizing the corral geometry with a combination of *simulated annealing* and *genetic algorithms*[14]. We find that i) it is possible to design quantum corrals with multiple mirages with both predefined positions and intensities once one has an accurate model of the scattering. ii) Our theory allow us to design quantum corrals that are particularly sensitive to the values of the phase shift, the only free parameter of the model. We show that it is possible to design structures that can be used to measure this phase shift.

II. DIRECT PROBLEM SOLUTION

A. Solving the scattering

We consider quantum corrals on the Cu(111) surface. Cu atoms on this surface form a triangular lattice with spacing $a = 2.55\text{\AA}$. This underlying triangular lattice defines also a triangular lattice for the equilibrium positions of the impurities that form the corral. The electronic structure of Cu(111) consist of a surface band with a Fermi energy ϵ_F laying 450 meV above the bottom of this band. We will treat the surface band as a two-dimensional-electron gas in the effective mass approximation. There is broad consensus [4, 6, 7, 8, 9, 15, 16] that the quantum mirages form as a result of the interplay between the impurities at the surface and this two dimensional surface band.

Several types of impurity atoms have been used to construct quantum corrals, examples

are Fe [3] and Co [4]. In all cases, the Fermi wave length of the electrons in the surface band is much larger than the spatial extension of the perturbation introduced by a single impurity atom. Therefore, an s-wave scattering approximation is good enough for the description of the electronic scattering by the impurities[16]. Accordingly, the impurities that form the corral are described by a single parameter being the s-wave phase shift δ .

For the case of N scatters located at positions $\{\mathbf{a}_i\}$ the retarded Green function G^{ret} of the system can be expressed in the following way[17]:

$$\begin{aligned} G^{\text{ret}}(\mathbf{r}, \mathbf{r}') = & G_0^{\text{ret}}(\mathbf{r}, \mathbf{r}') + & (1) \\ & + \sum_{ij} G_0^{\text{ret}}(\mathbf{r}, \mathbf{a}_i) [1/t - \mathbf{G}'_0]_{ij}^{-1} G_0^{\text{ret}}(\mathbf{a}_j, \mathbf{r}') \end{aligned}$$

where $[\mathbf{G}'_0]_{ij} = (1 - \delta_{ij}) \times G_0^{\text{ret}}(\mathbf{a}_i, \mathbf{a}_j)$ and t is the t-matrix of the identical scatters; in terms of the phase shift δ , $t = i \frac{\hbar^2}{m^*} (e^{i2\delta} - 1)$, being m^* the effective mass ($m^* = 0.38m_e$). In two dimensions and within the effective mass approximation [18], $G_0^{\text{ret}}(\mathbf{r}, \mathbf{r}'; \omega) = \frac{m^*}{2\hbar^2} (Y_0(k|\mathbf{r} - \mathbf{r}'|) - iJ_0(k|\mathbf{r} - \mathbf{r}'|))$, $\hbar k = \sqrt{2m^*\omega}$. While this method can be equally efficient for any phase shift model, for the purpose of this study, we chose to set $\delta = i\infty$ (unless otherwise specified) which has been determined to produce the best fit of the experimental information for quantum corrals constructed with Fe atoms on the cooper surface[19].

Equation (1) provides a straightforward way to obtain the exact Green function after an $N \times N$ matrix inversion. For the typical number of scatters that can be experimentally handled ($N \simeq 90$) this method is fast enough to solve thousand of different atomic configurations in seconds, each of them representing one trial step.

The Green function contains all the information about the solution of the independent particle problem and can be used to compute, for example, the local density of states (LDOS):

$$\mathcal{D}(\mathbf{r}; \omega) = -\frac{1}{\pi} \text{Im} G^{\text{ret}}(\mathbf{r}, \mathbf{r}; \omega) \quad (2)$$

or the perturbation caused by additional atoms, in particular magnetic impurities.

Let us note that G^{ret} is a function of the atomic positions $\{\mathbf{a}_i\}$. In this work we address the question of which is the corral (i.e. the set $\{\mathbf{a}_i\}$) that gives predefined couplings between magnetic impurities by means of modulating the RKKY interaction.

B. RKKY interaction in two dimensions

The exchange interaction of a magnetic impurity at coordinate \mathbf{R}_1 with an electron gas with coupling constant J_1 is described by the Hamiltonian:

$$H_{\text{imp}} = -J_1 \mathbf{S}_1 \cdot \psi^\dagger(\mathbf{R}_1) \boldsymbol{\sigma} \psi(\mathbf{R}_1) \quad (3)$$

where \mathbf{S}_1 describes the impurity spin, $\boldsymbol{\sigma} = (\sigma_x, \sigma_y, \sigma_z)$ are the Pauli matrices and $\psi^\dagger(\mathbf{r}) = (\psi_\uparrow^\dagger(\mathbf{r}), \psi_\downarrow^\dagger(\mathbf{r}))$ describes the electron field.

If a second magnetic impurity with spin \mathbf{S}_2 is placed at \mathbf{R}_2 , the effective impurity-impurity coupling mediated by the electron gas can be written as:

$$H_{12} = -\mathcal{J}_{12} \mathbf{S}_1 \cdot \mathbf{S}_2 \quad (4)$$

with

$$\mathcal{J}_{12} = \frac{4J_1 J_2}{\pi} \int d\omega f(\omega) \text{Im}[G_\downarrow^{\text{ret}}(\mathbf{R}_1, \mathbf{R}_2; \omega) G_\uparrow^{\text{ret}}(\mathbf{R}_2, \mathbf{R}_1; \omega)]. \quad (5)$$

where J_2 is the coupling of the second impurity with the electron gas, $f(\omega)$ is the Fermi function and $G_\sigma^{\text{ret}}(\mathbf{r}, \mathbf{r}'; \omega)$ is the retarded Green function for electrons with spin σ .

In general, to lowest order, the magnetic behavior of a collection of impurities at coordinates $\{\mathbf{R}_i\}$ is given by the following Hamiltonian:

$$H = \sum_{\langle ij \rangle} -\mathcal{J}_{ij} \mathbf{S}_i \cdot \mathbf{S}_j \quad (6)$$

where the summation is done over all impurity pairs. The exchange parameters \mathcal{J}_{ij} can be written as $\mathcal{J}_{ij} = J_i J_j C(\mathbf{R}_i, \mathbf{R}_j)$ with the correlation function $C(\mathbf{R}_i, \mathbf{R}_j)$ given by

$$\begin{aligned} C(\mathbf{R}_i, \mathbf{R}_j) &= \frac{4}{\pi} \int d\omega f(\omega) \text{Im}[G_\downarrow^{\text{ret}}(\mathbf{R}_i, \mathbf{R}_j; \omega) G_\uparrow^{\text{ret}}(\mathbf{R}_j, \mathbf{R}_i; \omega)] \\ &= -\frac{4}{\pi} \int_{-\infty}^{\epsilon_F} d\omega \text{Im}[G^{\text{ret}}(\mathbf{R}_i, \mathbf{R}_j; \omega)^2] \end{aligned} \quad (7)$$

The second line is obtained after assuming zero temperature, using the relations $G_\downarrow^{\text{ret}}(\mathbf{R}_1, \mathbf{R}_2; \omega) = (G_\downarrow^{\text{adv}}(\mathbf{R}_2, \mathbf{R}_1; \omega))^*$ and taking spin independent Green functions, this is exact in the absence of spin-orbit coupling and external magnetic fields. From here on we drop the spin index in the Green functions. The major contribution to the integral of

equation (7) comes from states near the Fermi energy[20], i.e. from $\text{Im}[G^{\text{ret}}(\mathbf{R}_i, \mathbf{R}_j; \epsilon_F)^2]$ [9, 20]. For the sake of avoiding the time consuming integration of Eq. (7) in the numerical method, we use the dominant contribution from the Fermi level:

$$C_{\epsilon_F}(\mathbf{R}_i, \mathbf{R}_j) = -\frac{4}{\pi} \text{Im} [G^{\text{ret}}(\mathbf{R}_i, \mathbf{R}_j; \epsilon_F)^2] \quad (8)$$

In the free surface, the RKKY interaction is oscillatory with a power law decay $1/|\mathbf{R}_i - \mathbf{R}_j|^2$. In the presence of an appropriate surrounding corral this interaction can be enhanced and focused[9]. In this work we exploit the fact that the correlation $C_{\epsilon_F}(\mathbf{R}_i, \mathbf{R}_j)$ can be controlled by changing the shape of the quantum corral, i.e. the RKKY interaction can be controlled by the quantum corral design.

Also, this correlation function (8) can be shown to be proportional to the perturbation in the *LDOS* at point \mathbf{R}_2 produced by a non magnetic impurity located at \mathbf{R}_1 [$\delta\mathcal{D}(\mathbf{R}_2, \mathbf{R}_1)$]. Therefore, to linear order, the search of magnetic mirages in the spin density is the same than the search of mirages in $\mathcal{D}(\mathbf{R}_2, \mathbf{R}_1)$; extending the scope of this work to the case where the perturbation is non magnetic but still localized in space.

III. THE INVERSE PROBLEM

Suppose that N impurities can fit in a lattice with spacing a , and we restrict them to a square with side l . The total number of possible configurations (including open geometries) is the combinatorial $n = (l/a)^2! / ((l/a)^2 - N)!N!$. For a typical system of $N = 30$, $a = 2.5\text{\AA}$ and $l = 100\text{\AA}$, $n \simeq 10^{64}$. Therefore, it is impossible to study all these configurations within reasonable times. Moreover, in the case of quantum corrals, most measurable quantities are expected to be non-smooth-multiple-valley functions of the $2N$ coordinates of the impurities due to the appearance and disappearance of resonant states for different configurations of the quantum corral (usually close-shaped corrals produce sharp resonances at discrete energies[3]). Therefore with a simple relaxation scheme, the system may be trapped in local minima of the multiple-valley function. Accordingly, more sophisticated non deterministic methods are required.

In spite of this large number of configurations, for most practical applications it is possible to avoid covering all the configuration space. At the same time, it is possible to find good enough solutions than can be improved systematically.

A. Simulated annealing

The simulated annealing algorithm [14, 21] is a quite general method to obtain minima of complicated functions of a large number of variables. In order to use a simulated annealing method we must define first a cost function $E(\{\mathbf{a}_i\})$. The cost function is simply a mathematical expression that quantifies the desired physical properties of the system; being minimum when the target is reached and maximum if undesired properties are present. Accordingly, the cost functions used in this work depend on one or more correlation functions. Several examples will be discussed in the applications below.

Once the cost function $E(\{\mathbf{a}_i\})$ is defined and a random initial configuration is chosen, the simulated annealing algorithm consists[22] in generating *random trial steps* and accepting them with a probability chosen following the Metropolis algorithm:

$$P(\Delta E) = \begin{cases} 1 & \text{if } \Delta E \leq 0 \\ \exp(-\Delta E/T) & \text{if } \Delta E > 0 \end{cases} \quad (9)$$

where ΔE is the change on the cost function in the trial step and T is a *fictitious temperature*. At each trial step the coordinates of the atoms of the corral are allowed to move in a triangular lattice representing the Cu(111) surface. In the annealing algorithm this *Metropolis dynamics* is repeated while T is gradually reduced[21]. This process allows the system to sample the space of variables, staying longer times near better global minimum as T diminishes. At $T = 0$, only favorable ($\Delta E < 0$) steps are allowed to take place but at finite T the system has the opportunity to escape from local minima. Eventually, if the fictitious temperature decreases slowly enough, the result will be a global or at least a good minimum. A particular property of the present system is, however, that for some parameters, as the quality of the minimum increases, the amplitude of the barriers grows. Therefore, rather than reducing the temperature, we smoothly adjust it continuously so as to maintain a target number of accepted changes. This implies that, in our case, as the cost function improves, the temperature rises. Finally, instead of reducing the fictitious temperature, as in the general simulated annealing case, we slowly reduce the target of accepted changes[14].

The rate of this reduction and how to define a cost function for a particular problem is in general a matter of trial and error and is not unique. Several examples for different situations will be given.

B. Genetic algorithm

Due to the presence of resonances, the performance of the simulated annealing decreases as better solutions are found or as a more complicated cost functions are introduced. Since we are actually looking for a big resonance, we have to consider a complementary method to optimize the configurations further. In order to further improve the optimization we combined simulated annealing with another Monte Carlo technique which is sometimes more robust, a *genetic algorithm*[14]. The genetic algorithm is a learning model which derives from an analogy with *evolution* process in nature.

In our case, for the quantum corral problem, we have designed a genetic algorithm that starts with a *population* of different corral configurations, termed *individuals*. In order to use genetic algorithms, one must define also a cost function (that we choose to be the same one used in the simulated annealing). The proposed cost function is evaluated for each individual of the population. The evaluation of each individual determines its probability to survive to the next *generation*. Statistically only the fittest (lowest cost function) are chosen to survive, those which are eliminated are replaced by the *offspring* resulting from mating survivors. In our case, we constructed the configuration of the corrals of the offspring as a random combination of the configurations of the corrals of the surviving parents. Accordingly, the offsprings keep geometrical similarities with their parents. In the general case of a genetic algorithm, a random mutation[14] is applied to the offspring in order to maintain diversity in the population. In our case, we replace this random mutation step by a simulated annealing step for each individual described above. We record the configuration of each individual that reaches the lowest cost during the simulated annealing step and use it for the next iteration. This combined process allows us to move continuously from a pure simulated annealing to a pure genetic algorithm depending on the number of individuals in the genetic algorithm and temperature and steps in the simulated annealing. Once a new population of quantum corrals is generated, the process starts again retaining the fittest and eliminating the rest. This combined procedure was repeated until a good solution was found.

In Table I we provide the parameters used to obtain the results shown in the Figures 1 to 6.

Case	Number of impurities	Targeted change	Sa steps	GA steps	GA population	Cost function
1	60	1%	7×10^6	1	1	-9.7,
2	90	1%	5×10^6	1	1	-7.0
3	120	1%	100^a	10^3	50	-6.2

^afor each mutation

TABLE I: Parameters and results for each of the cases studied

IV. RESULTS

A. A single mirage case: Alternatives to the ellipse

Guided by intuition we may think (as many of us did) that the ellipse was the optimum shape for a corral to enhance a perturbation of an impurity located at one focus of the ellipse into the other focus. This intuitive though originates in an analogy with geometrical optics[6]. Unfortunately, the analogy is valid only partially because of the following reasons: i) for the characteristic length scales of quantum corrals, geometrical optics is not completely valid and non trivial effects can arise from multiple scattering and purely quantum interference ; ii) the impurities can not be freely placed on the surface, there is always an underlying lattice (e.g. triangular for Cu(111)) that restricts the possible locations of the corral atoms. This restriction can have non negligible consequences as pointed out in Ref. [16]. iii) There is no theoretical proof that the ellipse is the optimal configuration of corral atoms, furthermore, the exact shape could depend on the particular phase shift model chosen, i.e. on the specific nature of the corral atoms.

Given these facts, the following question arises: is there any better atomic configuration than the elliptical one?

To test our method in this simple case, the simulated annealing algorithm was instructed to maximize the quantity $C_{\epsilon_F}(\mathbf{R}_1, \mathbf{R}_2)$, i.e. to project a perturbation from \mathbf{R}_1 to \mathbf{R}_2 as efficiently as possible. The cost function was chosen to be simply $E_1 = -C_{\epsilon_F}(\mathbf{R}_1, \mathbf{R}_2)$.

The reflection symmetry at the x -axis was imposed on the corral impurities to simplify the problem. The distance between the spins at \mathbf{R}_1 and \mathbf{R}_2 was fixed to 140 Å to resemble

the experimental conditions.

Once the optimization procedure is completed, we plot the correlation function of equation (7). In Figure 1 we show the response function and the quantum corral resulting from our optimization process [see Table I case 1 for parameters]. We see in Fig. 1 that the minimum found presents some resemblances to the ellipse but new unexpected features also appear. First of all, the atoms of the corral tend to accumulate around the location of the perturbation and also around the location of the desired mirage. Atoms on the long sides have less importance and are placed in a less dense arrangement. This contrasts with the evenly spaced atoms of the early experimental setups [3, 4]. A second shell of impurities appears to be more efficient than a single shell to confine the electron gas and produces better mirages.

For comparison we have studied the family of con-focal ellipses that can be formed with the same number of equidistant impurities (being the perturbation at one focus and the mirage at the other). We find that the best mirage formed by the family is a factor 3 smaller than the one obtained with the structure shown in Fig. 1.

This comparison with the ellipse demonstrates the power of the optimization technique we have developed, finding an alternative and better configuration for the formation of single quantum mirage. In the rest of this paper we exploit this technique further to study more complex problems.

B. Design of a quantum corral to generate chosen couplings between three spins

Returning to the problem of constructing physically an arbitrary Hamiltonian [see Eq. (6)], suppose now that we want to build a quantum corral such that generates a *target magnetic Hamiltonian* of three impurities:

$$H_{\text{target}} = -\mathcal{J}\mathbf{S}_1 \cdot \mathbf{S}_2 - \mathcal{J}\mathbf{S}_1 \cdot \mathbf{S}_3 \quad (10)$$

i.e. only a selected set of pairs of the three spins are coupled. We arbitrarily choose the coordinates of the spins \mathbf{R}_1 , \mathbf{R}_2 and \mathbf{R}_3 to be in the vertexes of an equilateral triangle of side $d = 121$ Å. Note that i) Eq. (10) is a particular case of Eq. (6) where $\mathcal{J}_{23} = 0$ and $\mathcal{J}_{12} = \mathcal{J}_{23} = \mathcal{J}$; and ii) the target Hamiltonian has a different symmetry than the desired positions of the magnetic spins. That is, we require the magnetic couplings on two sides

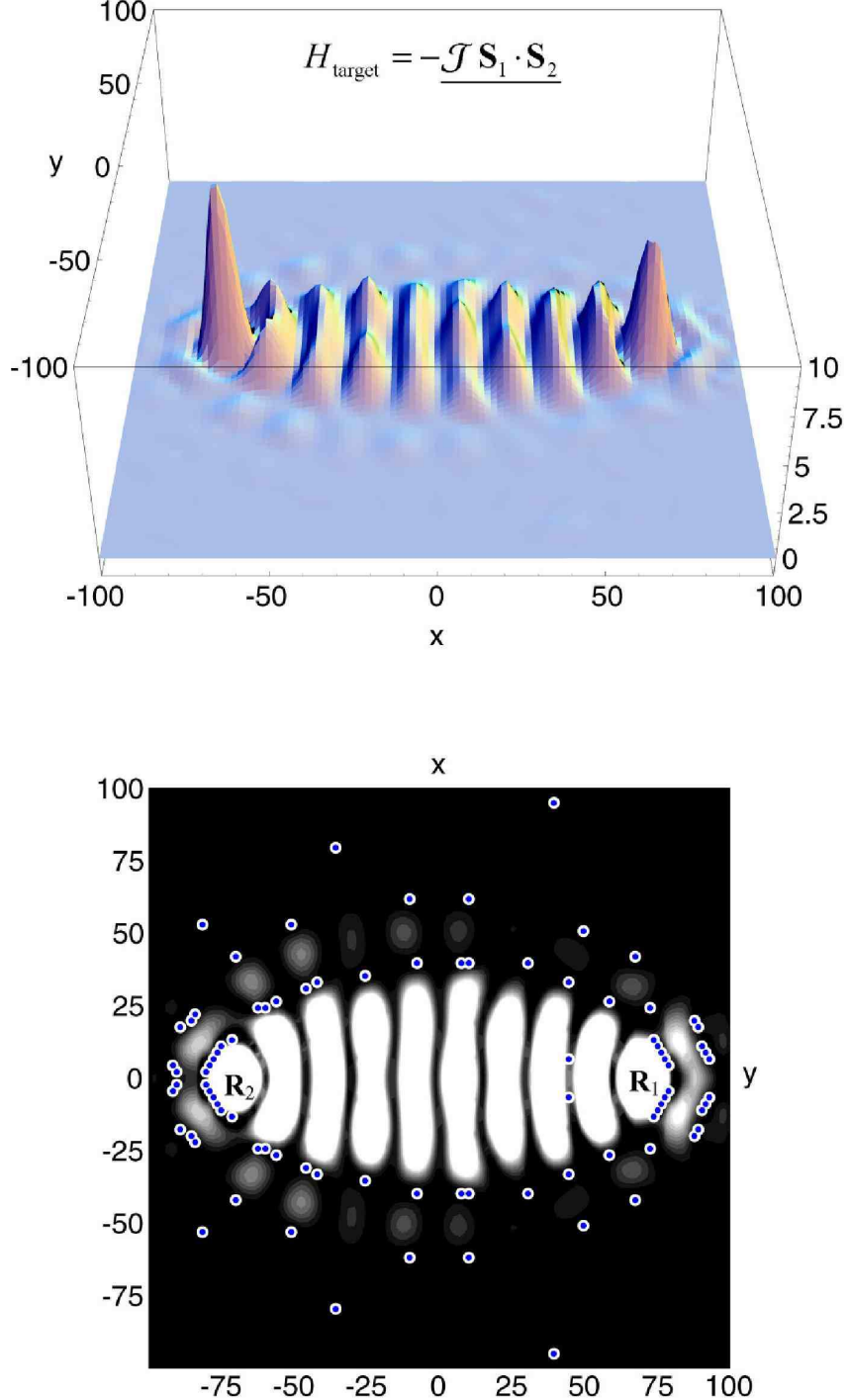


FIG. 1: (Color online). a) Magnetic response (linear order) to a spin located at \mathbf{R}_1 ($x = 70$ Å, $y = 0$) or quantum mirage formed as a result of an impurity at \mathbf{R}_1 . Distances are reported in Å. The corral is optimized to enhance the perturbation at point \mathbf{R}_2 ($x = -70$ Å, $y = 0$). The underlined term in Hamiltonian in the inset shows which magnetic interaction is associated with the correlation function displayed. b) Structure of $C_{\epsilon_F}(\mathbf{R}_1, \mathbf{r})$ below 5% of the largest peak. The design of the corral (white and blue dots) has been done with the Monte Carlo algorithm (see Case 1 in Table I).

of the triangle but not on the third. In terms of the electronic spin correlation function C_{ϵ_F} , this system requires $C_{\epsilon_F}(\mathbf{R}_2, \mathbf{R}_3) = 0$ and $C_{\epsilon_F}(\mathbf{R}_1, \mathbf{R}_2) = C_{\epsilon_F}(\mathbf{R}_1, \mathbf{R}_3)$ to be both as large as possible in order to enhance the interaction \mathcal{J} . We propose a cost function E_2 that favors these two requirements that is going to be minimized by the Monte Carlo techniques described earlier:

$$\begin{aligned} E_2 = & -C_{\epsilon_F}(\mathbf{R}_1, \mathbf{R}_2) - C_{\epsilon_F}(\mathbf{R}_1, \mathbf{R}_3) \\ & + |C_{\epsilon_F}(\mathbf{R}_1, \mathbf{R}_2) - C_{\epsilon_F}(\mathbf{R}_1, \mathbf{R}_3)| \\ & + |C_{\epsilon_F}(\mathbf{R}_2, \mathbf{R}_3)| \end{aligned} \quad (11)$$

The first two terms in Eq. (11) ensure that the interactions \mathcal{J} are enhanced; the third term is used to favor \mathcal{J}_{12} and \mathcal{J}_{13} to be equal; the last term penalizes the interaction \mathcal{J}_{23} . If the positions of the spins \mathbf{R}_1 , \mathbf{R}_2 and \mathbf{R}_3 are selected a priori and fixed, the cost function E_2 is just a function of the $2N$ coordinates $\{\mathbf{a}_i\}$ of the atoms forming the quantum corral. We also impose here the reflection symmetry along the x axis. The Monte Carlo algorithm automatically minimizes this cost function E_2 by varying $\{\mathbf{a}_i\}$. The parameters of the calculations can be taken from Table I case 2.

The resulting corral is shown in Fig. 2 and 3, the original requirements are efficiently achieved. In Fig. 2 we see that the optimum configuration found for the impurity atoms has dense focusing structures near the source of the perturbation and near the mirages. Amazingly, some atoms are automatically located in the middle of the corral to split the standing waves towards the “targets” at \mathbf{R}_2 and \mathbf{R}_3 . In Figure 3 we show the effect of a magnetic impurity at \mathbf{R}_3 which produces a large response at \mathbf{R}_1 but not at \mathbf{R}_2 [in contrast with the case of an impurity located at \mathbf{R}_1 (compare with Fig. 2)]. Let us emphasize that the corral is the same in Fig. 2 and 3, the difference is the position of the magnetic perturbation.

Comparison of Figures 2 and 3 shows that the RKKY interaction will induce couplings as initially designed. The resulting magnetization shows that \mathbf{S}_2 and \mathbf{S}_3 are not directly coupled while at the same time the interactions between \mathbf{S}_1 and \mathbf{S}_2 and between \mathbf{S}_1 and \mathbf{S}_3 are enhanced. We emphasize that the positions of the spins and the Hamiltonian chosen are arbitrary. We believe that we can find quantum corrals for a large number of targeted Hamiltonians using the same approach.

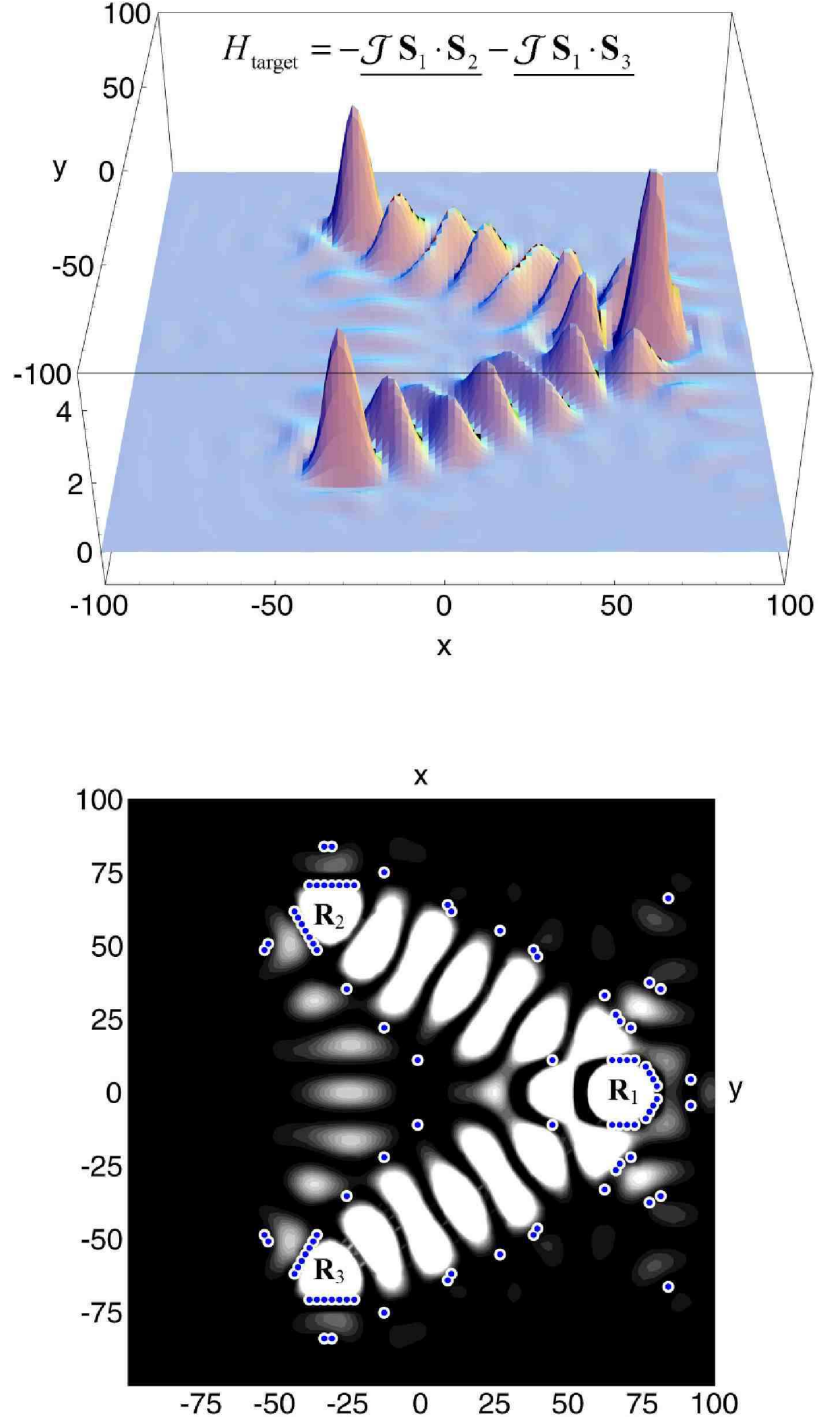


FIG. 2: (Color online) Quantum corral optimized to generate the spin Hamiltonian of Eq. (10). Response function $C_{\epsilon_F}(\mathbf{R}_1, \mathbf{r})$ due to a spin located at \mathbf{R}_1 ($x = 70$ Å, $y = 0$). Note the magnetic mirages at \mathbf{R}_2 and \mathbf{R}_3 . The underlined terms in the Hamiltonian in the inset show the magnetic interactions associated with the correlation function displayed. Same conventions and symbols as in Fig 1

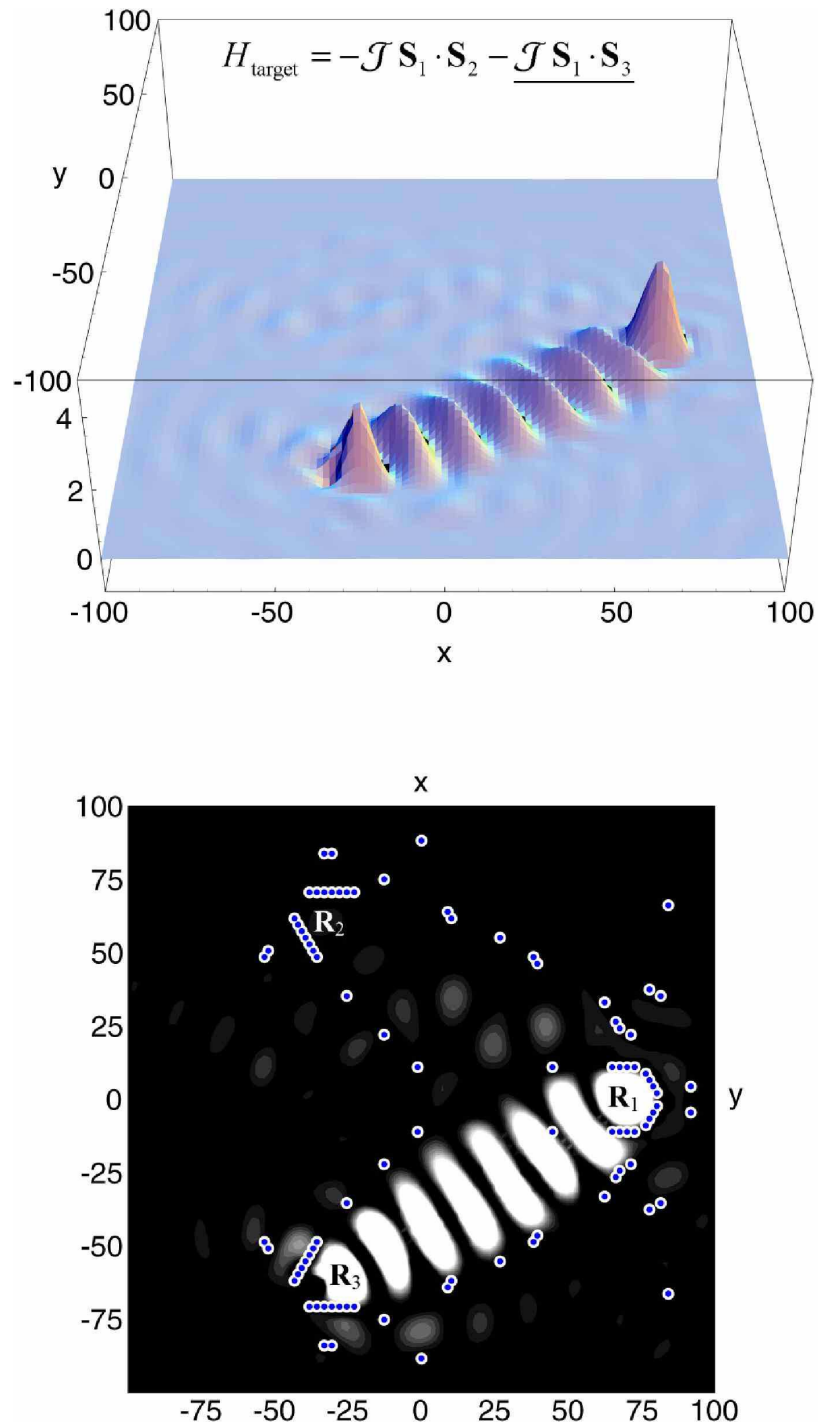


FIG. 3: (Color online) Quantum corral optimized to generate the spin Hamiltonian of Eq. (10). Magnetic response function $C_{\epsilon_F}(\mathbf{R}_3, \mathbf{r})$ due to a spin located at \mathbf{R}_3 . Same conventions and symbols as in Figs. 1 and 2

C. Four spins Hamiltonians

In this section we show the resulting design for four spins with a target Hamiltonian:

$$H_{\text{target}} = -\mathcal{J}\mathbf{S}_1 \cdot \mathbf{S}_3 - \mathcal{J}\mathbf{S}_2 \cdot \mathbf{S}_4 \quad (12)$$

where the positions of the spins form a square.

In order to achieve the target Hamiltonian of Eq. (12) by means of modulating the RKKY interaction, we chose the following cost function:

$$\begin{aligned} E_3 = & -C_{\epsilon_F}(\mathbf{R}_1, \mathbf{R}_3) - C_{\epsilon_F}(\mathbf{R}_2, \mathbf{R}_4) \\ & + |C_{\epsilon_F}(\mathbf{R}_1, \mathbf{R}_3) - C_{\epsilon_F}(\mathbf{R}_2, \mathbf{R}_4)| \\ & + |C_{\epsilon_F}(\mathbf{R}_1, \mathbf{R}_2)| \\ & + |C_{\epsilon_F}(\mathbf{R}_2, \mathbf{R}_3)| \\ & + |C_{\epsilon_F}(\mathbf{R}_3, \mathbf{R}_4)| \\ & + |C_{\epsilon_F}(\mathbf{R}_4, \mathbf{R}_1)| \end{aligned} \quad (13)$$

The first two terms were introduced to increase the interaction between spins at opposite vertexes; the role of the third term is to favor identical coupling between the two pairs of spins ($\mathcal{J}_{13} = \mathcal{J}_{24} = \mathcal{J}$, note that any difference will increase the cost function); the rest of the terms penalize the coupling between consecutive spins (in order to achieve that $\mathcal{J}_{12} = \mathcal{J}_{23} = \mathcal{J}_{34} = \mathcal{J}_{41} = 0$). For this case we impose symmetry along the “x” and “y” axes. The method for optimization is similar to the one used in the cases described above but in this case the genetic algorithm plays a more important role. The parameters of the calculations can be taken from Table I case 3.

The results of minimizing Eq. (13) are shown in Fig. 4 and 5. Figure 4 shows the spin density generated by a perturbation at \mathbf{R}_1 and Figure 5 the spin density when the magnetic perturbation is at \mathbf{R}_2 . Note in Fig. 4 that a magnetic mirage appears at \mathbf{R}_3 ($x = -70$ Å, $y = 0$) but neither at \mathbf{R}_2 ($x = 0, y = 70$ Å) nor at \mathbf{R}_4 ($x = 0, y = -70$ Å). Conversely in Fig. 5, the magnetic mirage forms at \mathbf{R}_4 ($x = 0, y = -70$ Å) but neither at \mathbf{R}_1 ($x = 70$ Å, $y = 0$) nor at \mathbf{R}_3 ($x = 0, y = -70$ Å). Therefore, the spin Hamiltonian formed by this structure has two pairs of spins interacting independently. Each pair of spins do not couple with the other pair, even though the interaction is mediated by an electron gas that is shared by both pairs. Such couplings have been recently achieved experimentally[23], here we present a structure

that achieves a similar objective where the mirages are much closer and couplings between crossing pairs are specifically avoided.

D. Optimization for other purposes: optimal corrals to determine phase shifts

Let us discuss for the moment the limitations of our approach. Our model describes the resonances in the densities of states in terms of an scattering theory which depends on a single parameter: the phase shift δ . The perturbation in the density of states due to single impurity [24] or an entire corral [19] has been used to measure the characteristic phase-shift of a particular type of impurity. We note, however, that such a procedure is not very sensitive to the phase shift and that might be the reason of some controversy in the literature[19, 25]. The origin of this lack of sensitivity comes from the fact that the systems fitted were not optimized to be sensitive to the phase shift. For example, dense and closed shaped corrals do not produce densities of states that is sensitive to the phase shift of the individual atoms of the corral. It is therefore our goal in this section to demonstrate the possibility of optimizing a quantum corral for the determination of the phase shift δ .

We first describe the optimization of a quantum corral geometry with the aim of measuring δ . Subsequently, we characterize the corral as an experimental device to measure phase shifts.

Let us first concentrate on Figure 2 that shows a corral optimized to obtain a couple of mirages at symmetric points \mathbf{R}_2 and \mathbf{R}_3 due to a perturbation at \mathbf{R}_1 . As we noted in Section II Eq. (8), within linear response, magnetic mirages are proportional to finite differences in the density of states under a paramagnetic perturbation [i.e. $C_{\epsilon_F}(\mathbf{R}_2, \mathbf{R}_1) \sim \delta \mathcal{D}(\mathbf{R}_2, \mathbf{R}_1)$] The latter have been measured experimentally.[4, 26]

As the corral in Figure 2 was forced to have reflection symmetry along the x axis, $\delta \mathcal{D}(\mathbf{R}_2, \mathbf{R}_1)$ and $\delta \mathcal{D}(\mathbf{R}_3, \mathbf{R}_1)$ are identical. However, if we place an additional impurity outside the x axis at a point \mathbf{R}_4 , the symmetry of the system is broken. A difference in the amplitudes of the mirages at \mathbf{R}_2 and \mathbf{R}_3 due to a perturbation at \mathbf{R}_1 will reflect the contribution of this single asymmetric impurity at \mathbf{R}_4 . Intuitively one would guess that the difference will be largest if we put R_4 at $(\mathbf{R}_1 + \mathbf{R}_2)/2$ in order to interfere with the coupling between \mathbf{R}_1 and \mathbf{R}_2 but not with the coupling between \mathbf{R}_1 and \mathbf{R}_3 . However, in order to help intuition, we optimized the corral further so as it gives a large difference

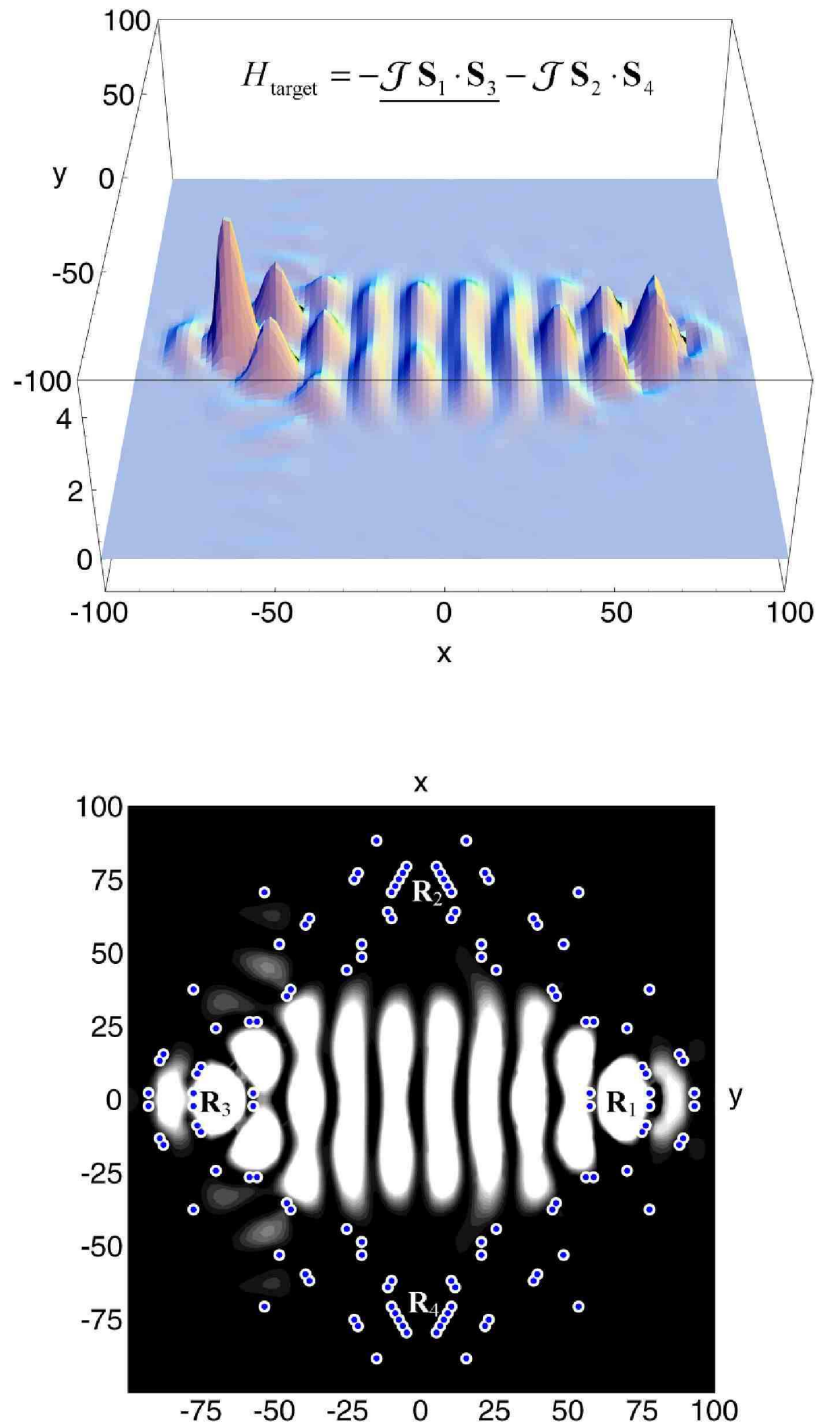


FIG. 4: Quantum corral optimized to generate the spin Hamiltonian of Eq. (12). Magnetic response function $C_{\epsilon_F}(\mathbf{R}_1, \mathbf{r})$ due to a spin at \mathbf{R}_1 ($x = 70$ Å, $y = 0$). Same conventions and symbols as in Fig. 1. Compare to Fig. 5.

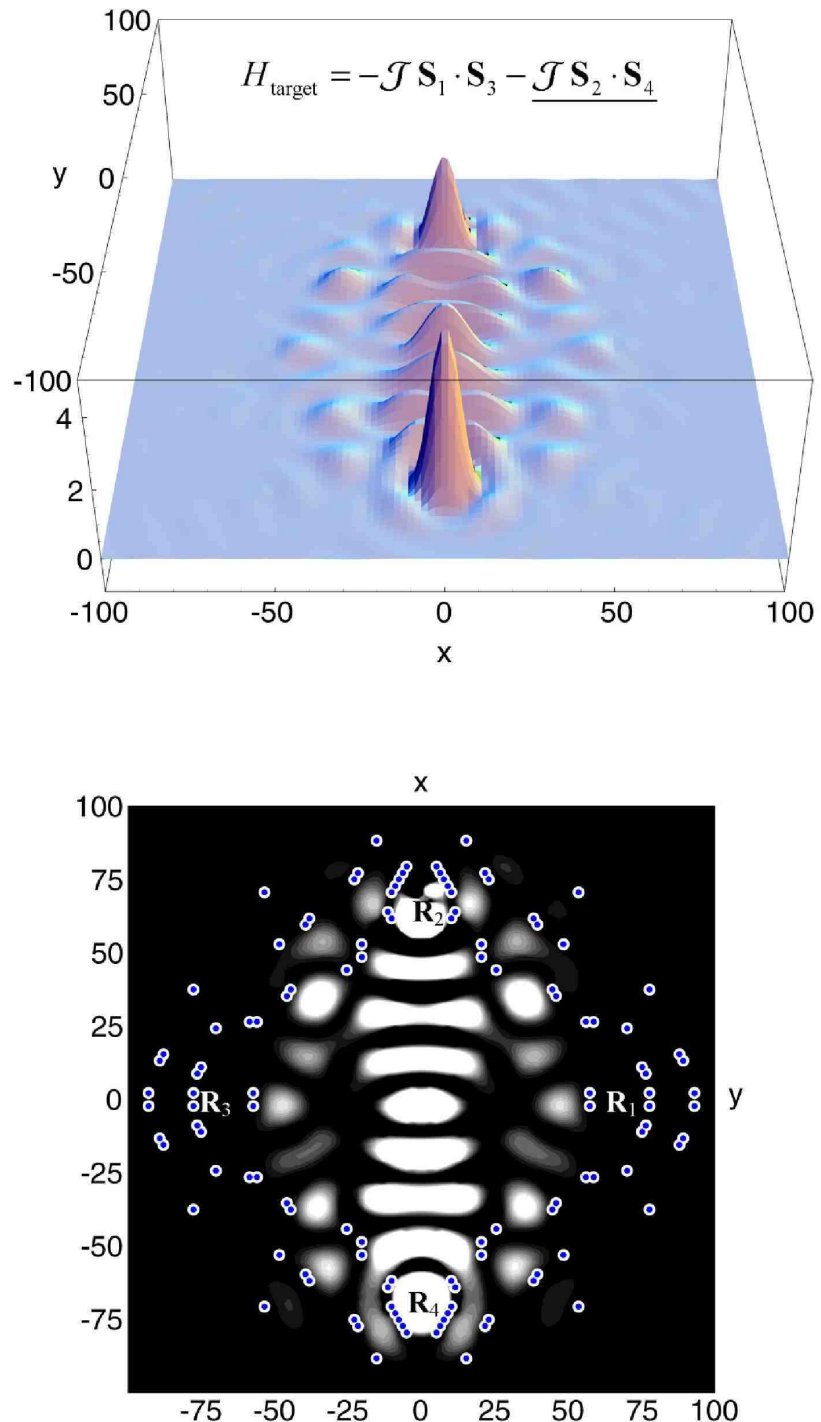


FIG. 5: (Color online) Quantum corral optimized to generate the spin Hamiltonian of Eq. (12). Magnetic response function $C_{\epsilon_F}(\mathbf{R}_2, \mathbf{r})$ due to a spin at \mathbf{R}_2 ($x = 0$, $y = 70$ Å). Same conventions and symbols as in Fig 1. Compare to Fig. 4.

$\Delta^2 = \delta\mathcal{D}(\mathbf{R}_2, \mathbf{R}_1) - \delta\mathcal{D}(\mathbf{R}_3, \mathbf{R}_1)$ when there is a fix impurity at \mathbf{R}_4 while the rest of the impurities have reflection symmetry along the x axis and we perturbed the system with an impurity at \mathbf{R}_1 . With that goal we design the following cost function:

$$\begin{aligned} E_4 = & -C_{\epsilon_F}(\mathbf{R}_2, \mathbf{R}_1) - C_{\epsilon_F}(\mathbf{R}_3, \mathbf{R}_1) + |C_{\epsilon_F}(\mathbf{R}_2, \mathbf{R}_3)| \\ & - |(C_{\epsilon_F}(\mathbf{R}_2, \mathbf{R}_1) + C_{\epsilon_F}(\mathbf{R}_2, \mathbf{R}_4)) \\ & - (C_{\epsilon_F}(\mathbf{R}_3, \mathbf{R}_1) + C_{\epsilon_F}(\mathbf{R}_3, \mathbf{R}_4))| \times 0.5. \end{aligned} \quad (14)$$

The first part of Eq. (14) is the same as Eq. (11). The second part is maximum when there is a big difference in the mirages at \mathbf{R}_1 and \mathbf{R}_3 when there is an additional impurity at \mathbf{R}_4 (treated in the limit of linear response). The weight factor (0.5) in the last term in Eq. (14) controls the relative importance of large mirages vs. large differences.

After the simulated annealing procedure, the corral obtained with the cost function (14) is similar to the one obtained in Fig. 2 because the cost function (11) and (14) are similar [27]. Let us concentrate on the amplitudes of the mirages ($\delta\mathcal{D}$) as a function of the phase shift δ of the impurities of the corral. In the inset of Fig. 6(a) we show the amplitude of the mirage (either at \mathbf{R}_2 or \mathbf{R}_3) due to a perturbation at \mathbf{R}_1 for the symmetric case (without the impurity at \mathbf{R}_4) as a function of the phase shift parameter δ . $\delta\mathcal{D}(\mathbf{R}_2, \mathbf{R}_1)$ is measured in units of the density of states at the Fermi level of the unperturbed electron gas. We see that the amplitude of the mirages grows monotonically with δ saturating around 2.5. While the magnitude of $\delta\mathcal{D}$ could be used to determine, by comparison with an experiment, the parameter δ , that would be not enough to verify the validity of the model used to construct the corral. As for a different model (i.e. a real phase shift) we would find a different way to fit the same data: we need at least two measurements to verify the validity of a model with a single free parameter. In Figure 6 (black line) we plot Δ^2 when there is an additional impurity at \mathbf{R}_4 as a function of a common phase shift δ . The value of Δ^2 also increases monotonically with δ but saturates earlier (around $\delta = 1$). Note that the difference between the two mirages can be of the order of 20 % of the density of states at the Fermi level. Therefore, we believe that the contribution of a single impurity can be measured within experimental resolution, providing alternative data to corroborate the present surface scattering model.

Finally, let us characterize this double mirage structure as an experimental device to measure surface scattering cross sections or phase shifts of arbitrary impurities. Let us

assume that the surface of Cu is doped mainly with type one atom (lets say Co) but also that there are additional minority impurities on the surface available. Let us say that we are not even sure what is the phase shift of our majority impurity. The following question arises: is this quantum corral made of impurities of unknown phase shift good enough to estimate the phase shifts of any other impurity?. The doted lines lines in Figure 6 have been drawn assuming that the impurities of the corral have a phase shift δ of 0.5 1 and 2 as a function of the phase shift δt of a *different* the impurity in \mathbf{R}_4 and a perturbation with phase shift δ at \mathbf{R}_1 . We see that Δ^2 is quite insensitive to the phase shift of the impurities of the corral, suggesting that only the geometry chosen for confinement determines Δ^2 . Therefore, a single quantum corral device can be used to “measure” the phase shift of every impurity in the periodic table in spite of the uncertainly in the knowledge of the phase shift of the impurities in the corral. Note finally, that the cost function was build such that the corral was very sensitive to small perturbations at R_4 . Therefore, our proposed “experimental device” is very sensitive to small phase shifts and saturates faster for larger ones than the amplitude of the mirages (see inset). Alternatively one might have chosen a different cost function to selectively measure higher vales of δt .

V. DISCUSSION AND CONCLUSIONS

We have demonstrated the possibility to design theoretically quantum corrals with multiple quantum mirages. In this work we have overcome the problem posed by resonances and multiple scattering in quantum corrals that give rise to a both a very large configuration space and a very irregular response function. This response function structure makes deterministic algorithms fail to find good minima. The automated design algorithm is useful to attack the inverse problem specially in cases where the intuition fails or gives poor answers. Instead of covering the huge space of all possible configurations, we propose a non deterministic method to explore the possible configurations. For the examples covered here, 10^6 steps were enough to optimize the structure.

The enhancement of magnetic interactions due to electronic confinement together with the automatic design of the quantum corrals allows us to tailor structures that generate a variety of spin Hamiltonians involving several magnetic neighbors. We demonstrate in this work that it is in principle possible to design quantum corrals such as the geometry of

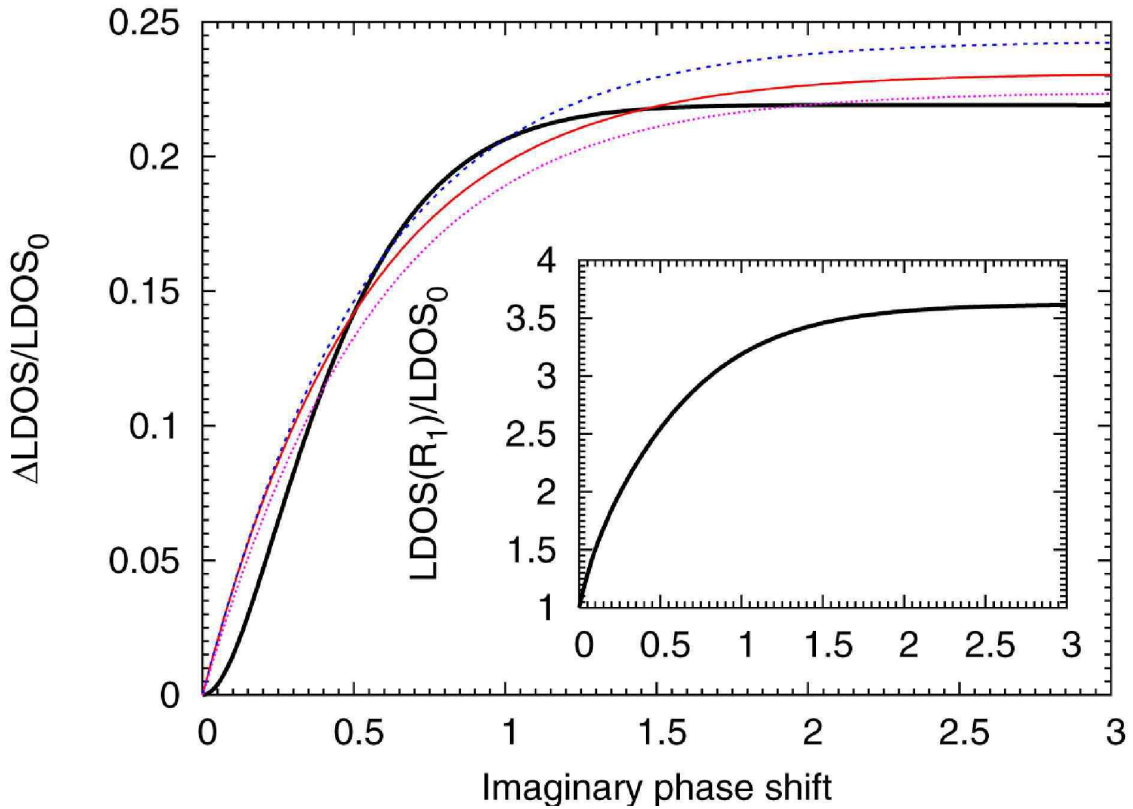


FIG. 6: (Color online) $\Delta^2 = \delta\mathcal{D}(\mathbf{R}_2) - \delta\mathcal{D}(\mathbf{R}_3)$ difference produced by an additional impurity at \mathbf{R}_4 as a function of the phase shift of all impurities (full line), or assuming a fixed value of the phase shift of the corral (red $\theta = 0.5i$, blue $\theta = 1i$, magenta $\theta = 2i$) but varying the phase shift of the impurity at \mathbf{R}_4 . Units in density of state of free electron gas.

the system produces magnetic images at predetermined points. This opens the possibility to actually construct experimentally magnetic Hamiltonians of any sort imposed a priori. This could open a path to study experimentally a number of Hamiltonians which have been subject of intense theoretical research along the years. In particular one could study one dimensional spin Hamiltonians where there are analytical solutions. Such ability to construct Hamiltonians might be relevant in the context of quantum computation. We note in passing that one of the proposals to build quantum computers is based on the interaction of nuclear spins mediated by an electron gas[1]. The physical realization of prescribed Hamiltonians is a necessary step in quantum computation. The measurement of isolated spins in quantum corrals has been experimentally demonstrated. [4, 26] The exchange Heisenberg coupling was theoretically shown to be suitable for quantum computation[2]. The combination of these

two ingredients and our method to design optimum quantum corrals opens the possibility to actual realizations of quantum computers with spins on a surface. But, in addition, Quantum Computation requires the ability to turn interactions on and off [2]. In principle the interactions between impurities can be turned on and off by changing the position of the Fermi level in the surface band with respect to the bulk band. While the control of the Fermi level might be difficult in copper surfaces it is much easier in semiconductor quantum wells.

VI. ACKNOWLEDGMENTS

The authors would like to thank Giulia Galli for support comments and suggestions and to Roy Pollock for a critical reading of the manuscript. This work was performed under the auspices of CONICET Argentina and of the U.S. Dept. of Energy at the University of California/Lawrence Livermore National Laboratory under contract no. W-7405-Eng-48.

- [1] B. E. Kane, *Nature* **393**, 133 (1998).
- [2] D. P. DiVincenzo, D. Bacon, J. Kempe, G. Burkard, and K. B. Whaley, *Nature* **408**, 339 (2000).
- [3] M. F. Crommie, C. P. Lutz, and D. M. Eigler, *Science* **264**, 218 (1993).
- [4] H. C. Manoharan, C. P. Lutz, and D. M. Eigler, *Nature* **403**, 512 (2000).
- [5] A. C. Hewson, *The Kondo Problem to Heavy Fermions* (Cambridge University Press, 1997).
- [6] O. Agam and A. Schiller, *Physical Review Letters* **86**, 484 (2001), URL <http://link.aps.org/abstract/PRL/v86/p484>.
- [7] A. A. Aligia, *Physical Review B (Condensed Matter and Materials Physics)* **64**, 121102 (pages 4) (2001), URL <http://link.aps.org/abstract/PRB/v64/e121102>.
- [8] K. Hallberg, A. A. Correa, and C. A. Balseiro, *Physical Review Letters* **88**, 066802 (pages 4) (2002), URL <http://link.aps.org/abstract/PRL/v88/e066802>.
- [9] A. A. Correa, K. Hallberg, and C. A. Balseiro, *Europhysics Letters* **58**(6), 899 (2002).
- [10] G. Chiappe and A. A. Aligia, *Physical Review B (Condensed Matter and Materials Physics)* **66**, 075421 (pages 5) (2002), URL <http://link.aps.org/abstract/PRB/v66/e075421>.
- [11] A. Franceschetti and A. Zunger, *Nature* **402**, 60 (1999).
- [12] J. D. Lohn, W. F. Kraus, and S. P. Colombano, *Proc. of the Fourth International Conference on Evolvable Systems* pp. 236–243 (2001), URL <http://ic.arc.nasa.gov/people/jlohn/Papers/ices2001.pdf>.
- [13] A. Globus, M. Menon, and E. Ricks, *Proc. of the 2003 Nanotechnology Conference and Trade Show* (2003), URL http://ic.arc.nasa.gov/projects/esg/publications/globus_papers/NanoTech2003/paper_02.pdf.
- [14] E. Aarts and J. K. Lenstra, eds., *Local search in combinatorial optimization* (Princeton University Press, 1997).
- [15] D. Porras, J. Fernández-Rossier, and C. Tejedor, *Physical Review B* **63**, 155406 (2001).
- [16] G. A. Fiete and E. J. Heller, *Reviews of Modern Physics* **75**, 933 (pages 16) (2003), URL <http://link.aps.org/abstract/RMP/v75/p933>.
- [17] L. S. Rodberg and R. M. Thaler, *Introduction to the Quantum Theory of Scattering (Pure and Applied Physics, Vol 26)* (Academic Press, 1967).

- [18] E. N. Economou, *Green's Function in Quantum Physics* (Springer Verlag, 1990).
- [19] E. J. Heller, M. F. Crommie, C. P. Lutz, and D. Eigler, *Nature* **369**, 464 (1994).
- [20] C. Kittel, *Quantum Theory of Solids* (John Wiley & Sons, New York, 1963).
- [21] W. H. Press, B. P. Flannery, S. A. Teukolsky, and W. T. Vetterling, *Numerical Recipes in C : The Art of Scientific Computing* (Cambridge University Press, 1992).
- [22] M. R. A. T. N. Metropolis, A.W. Rosenbluth and E. Teller, *J. Chem. Phys.* pp. 1087–1092 (1953).
- [23] D. M. Eigler, C. P. Lutz, M. F. Crommie, H. C. Manoharan, H. A. J., and J. A. Gupta, *Phil. Trans. R. Soc. Lond. A* (2004).
- [24] M. A. Schneider, L. Vitali, N. Knorr, and K. Kern, *Physical Review B* **65**, 121406 (2002).
- [25] H. K. Harbury and W. Porod, *Physical Review B* **53**, 15455 (1996).
- [26] C. Durkan and M. E. Welland, *Applied Physics Letter* **80**, 458 (2002).
- [27] Please contact authors for coordinates.